



Synergistic effects of drought and deforestation on the resilience of the  
south-eastern Amazon rainforest

Staal, A., Dekkers, S., Hirota Magalhaes, M., & van Nes, E. H.

This is a "Post-Print" accepted manuscript, which has been published in "Ecological  
Complexity"

This version is distributed under a non-commercial no derivatives Creative Commons



([CC-BY-NC-ND](#)) user license, which permits use, distribution, and reproduction in any medium, provided the original work is properly cited and not used for commercial purposes. Further, the restriction applies that if you remix, transform, or build upon the material, you may not distribute the modified material.

Please cite this publication as follows:

Staal, A., Dekkers, S., Hirota Magalhaes, M., & van Nes, E. H. (2015). Synergistic effects of drought and deforestation on the resilience of the south-eastern Amazon rainforest. *Ecological Complexity*, 22, 65-75.  
<https://doi.org/10.1016/j.ecocom.2015.01.003>

1 Synergistic effects of drought and deforestation on the resilience of the south-eastern Amazon  
2 rainforest

3  
4 Arie Staal<sup>a,b</sup>, Stefan C. Dekker<sup>b</sup>, Marina Hirota<sup>c</sup>, Egbert H. van Nes<sup>a</sup>

5  
6 <sup>a</sup> Aquatic Ecology and Water Quality Management Group, Wageningen University, P.O. Box  
7 47, 6700 AA, Wageningen, The Netherlands

8  
9 <sup>b</sup> Department of Environmental Sciences, Copernicus Institute for Sustainable Development,  
10 Utrecht University, P.O. Box 80115, 3508 TC Utrecht, The Netherlands

11  
12 <sup>c</sup> Department of Physics, Federal University of Santa Catarina, P.O. Box 476, 88040-970,  
13 Florianópolis, Brazil

14  
15 Corresponding author: Arie Staal

16 Phone: +31 317 482689 / Fax: +31 317 484411

17 E-mail addresses: arie.staal@wur.nl (A. Staal), s.c.dekker@uu.nl (S.C. Dekker),

18 marina.hirota@ufsc.br (M. Hirota), egbert.vannes@wur.nl (E.H. van Nes)

**Abstract** The south-eastern Amazon rainforest is subject to ongoing deforestation and is expected to become drier due to climate change. Recent analyses of the distribution of tree cover in the tropics show three modes that have been interpreted as representing alternative stable states: forest, savanna and treeless states. This situation implies that a change in environmental conditions, such as in the climate, could cause critical transitions from a forest towards a savanna ecosystem. Shifts to savanna might also occur if perturbations such as deforestation exceed a critical threshold. Recovering the forest would be difficult as the savanna will be stabilized by a feedback between tree cover and fire. Here we explore how environmental changes and perturbations affect the forest by using a simple model with alternative tree-cover states. We focus on the synergistic effects of precipitation reduction and deforestation on the probability of regime shifts in the south-eastern Amazon rainforest. The analysis indicated that in a large part of the south-eastern Amazon basin rainforest and savanna could be two alternative states, although massive forest dieback caused by mean-precipitation reduction alone is unlikely. However, combinations of deforestation and climate change triggered up to 6.6 times as many local regime shifts than the two did separately, causing large permanent forest losses in the studied region. The results emphasize the importance of reducing deforestation rates in order to prevent a climate-induced dieback of the south-eastern Amazon rainforest.

**Keywords** bistability, climate change, critical transitions, fire, regime shifts, tipping points

## 1. Introduction

Every year, large areas of rainforest are being deforested in the Amazon. In addition, increased drought is expected to affect parts of the rainforest over the course of the coming century (Malhi et al., 2008). In recent years there has been much interest in the question whether climate change and deforestation may cause the forest to die back, or even collapse due to positive feedbacks that cause alternative stable states (Cox et al., 2000; Lenton et al., 2008; Nepstad et al., 2008; Malhi et al., 2009; Davidson et al., 2012). Analyses of MODIS satellite data of tree cover by Hirota et al. (2011) and Staver et al. (2011b) have added new evidence for alternative states (Scheffer and Carpenter, 2003) by showing that the frequency distributions of tree cover in the tropics have three modes, which roughly correspond to a treeless ecosystem, savanna (tree-grass mosaics) and forest. The probability of finding these modes depends non-linearly on mean annual precipitation (MAP) (Hirota et al., 2011).

The existence of alternative stable states implies that an ecosystem can be in several alternative states under the same external conditions. When the system is perturbed slightly, it will return to the stable equilibrium. However, when a perturbation exceeds a certain size, the system will move to an alternative equilibrium. Such a regime shift can also occur when the environmental conditions cross a fold bifurcation point, often called ‘tipping point’ (Scheffer et al., 2009). Restoring the conditions that were present prior to the shift requires a larger change in environmental conditions, a phenomenon called hysteresis. We refer to these regime shifts as critical transitions (Scheffer, 2009). A slow change in environmental conditions can make a system more vulnerable for a regime shift. The maximum possible perturbation without causing a regime shift is defined by as a system state’s (ecological) resilience (Holling, 1973).

There is increasing evidence that fire is the mechanism for creating alternative stable states of tropical rainforest and savanna (Staver et al., 2011b; Hoffmann et al., 2012; Murphy

and Bowman, 2012). Savannas are open, grassy landscapes, which can be maintained by frequent fires. As fire-exclusion experiments (e.g. Moreira, 2000) have shown, fires can prevent the establishment of forest when the climate would allow for its presence (Bond, 2008). Indeed, the grasses in savannas may fuel natural or anthropogenic fires, which kill forest tree species (Hoffmann et al., 2012). Fires are sometimes seen as external disturbances maintaining an unstable savanna regime (Sankaran et al., 2005). However, fires can be regarded as a self-stabilizing mechanism of savannas, as the low tree cover in savannas enhances fires. Closed-canopy forests, on the other hand, suppress fires through the creation of a humid understory microclimate (Uhl and Kauffman, 1990) and can thereby stabilize the forest state itself (Hoffmann et al., 2012; Murphy and Bowman, 2012). Fragmentation of the canopy results in a much higher vulnerability to fire. Both grasses invading the forest and trees killed by fire can fuel fires, making burned forest areas even more susceptible to burning (Cochrane et al., 1999; Brando et al., 2014). After a number of fires a savanna ecosystem may establish. Next to the internal feedbacks, also climatic conditions influence the probability of fire; the drier it is, the more intense fires tend to be (Pueyo et al., 2010), so the more likely a regime shift from forest to savanna would become. On centennial to millennial time scales, however, these shifts need not be permanent. For an African savanna, for example, back-and-forth transitions between savanna and forest have been reported (Gil-Romera et al., 2010). Such repeated shifting between alternative stable states is called flickering (Scheffer, 2009).

Both deforestation and climate change in the Amazon are relatively severe in the drier, south-eastern part of the basin, an area characterized as the “arc of deforestation” (Aragão et al., 2007; Davidson et al., 2012; Coe et al., 2013). Therefore, in particular tree cover in the south-eastern Amazon can be expected to be out of equilibrium and vulnerable to future regime shifts, but the resilience of the forest is only poorly understood. Our objective was to assess how deforestation (defined as a reduction in tree cover; Sternberg, 2001) and climate

change (a reduction in mean annual precipitation) may interact to induce fire-mediated regime shifts from forest to savanna in the south-eastern Amazon. Current forest models are generally not suited for analyzing tipping point behavior, while there is a need for models that are (Reyer et al., 2015). Previous studies concerned with alternative stable states in the Amazon have mainly focused on a regional forest-precipitation feedback instead of the tree cover-fire feedback (Nobre and Borma, 2009). We present a simple model for tree cover in South America that includes the tree cover-fire feedback and was fitted to near-continent-wide satellite data. We use it to simulate deforestation- and climate change-induced regime shifts to savanna in the south-eastern Amazon rainforest.

## 2. Methods

### 2.1. The model

We adapted a simple tree-cover model by Van Nes et al. (2014). It can have three stable tree-cover states, corresponding to treeless, savanna and forest states, and has been fitted to satellite data of tree cover across the Earth's tropics. The model consists of a logistic growth function for the expansion of tree cover  $T$  (fraction) to carrying capacity  $K$  (fraction) and two loss terms. The expansion rate depends on precipitation  $P$  (mm yr<sup>-1</sup>) and saturates at  $r_m$  (yr<sup>-1</sup>) with a half saturation of  $h_P$  (mm yr<sup>-1</sup>). The first loss term includes increased mortality at low tree-cover densities, called an Allee effect. This represents the facilitative effect of adult trees on tree-seedling establishment in the seedling's competition with grasses (Holmgren et al., 1997; Baudena et al., 2010). The Allee-effect-induced loss rate decreases from  $m_A$  (yr<sup>-1</sup>) with  $T$  according to a Monod function with half saturation  $h_A$  (fraction). The growth function and Allee effect are given as:

$$\frac{dT}{dt} = \frac{P}{h_P + P} r_m T \left(1 - \frac{T}{K}\right) - m_A T \frac{h_A}{T + h_A} \quad (1)$$

115

116 The Van Nes et al. (2014) model also includes a second mortality term that mimics the effect  
 117 of fire at intermediate tree cover. A Hill function describes the sigmoidal shape of the  
 118 negative relationship between tree cover and fire-induced mortality. Thus, fire depends solely  
 119 on tree cover in Van Nes et al. (2014) and not on environmental conditions. However, in  
 120 reality fire occurrence and intensity also depend on rainfall (Staver et al., 2011b). Therefore,  
 121 we adjusted the fire term accordingly for this paper, although we do not depart from the  
 122 simple approach of Van Nes et al. (2014). In this new model, fire-induced tree-cover  
 123 mortality depends on fire intensity  $I$ , whereby trees are resistant to low-intensity fires through  
 124 a Hill function. Fire intensity depends negatively and non-linearly on tree cover. This can be  
 125 thought of as representing the availability of fuel (grass), which is determined by the openness  
 126 of the landscape. Although a fragmented canopy may affect tree cover in several ways  
 127 (Cumming et al., 2012), this landscape openness mainly promotes the continuity of the grassy  
 128 (i.e. non-forested) portion of the landscape such that above a certain threshold of this  
 129 continuity fires can percolate through the landscape (Archibald et al., 2009; Pueyo et al.,  
 130 2010; Hoffmann et al., 2012; Staver and Levin, 2012). Therefore,  $I$  depends on a variable  
 131 landscape continuity  $C(T)$ , which is a function of tree cover  $T$  through a saturating sigmoidal  
 132 function (Hill function). When  $T$  equals the half saturation  $h_C$  the largest change in  $C$  occurs.

133 Following the rationale that the moisture content of the fuel, and therefore its  
 134 flammability, depends on soil moisture (Hirota et al., 2010; Murphy and Bowman, 2012), fire  
 135 intensity  $I$  also depends on a soil moisture index  $SMI$ . This index depends on  $P$  via a  
 136 sigmoidal Hill function (Hirota et al., 2010; Staver and Levin, 2012). The choice for a  
 137 sigmoid is empirically supported by Bucini and Hanan (2007), who found that it could best  
 138 describe the relationship between mean annual precipitation (MAP) and tree cover in the

African savannas. Because our model represents processes on an annual basis, the fire-induced mortality is divided by a constant fire return interval  $FRI$ . The resulting differential equation for tree cover  $T$  (fraction) is as follows:

$$\frac{dT}{dt} = \frac{P}{h_P + P} r_m T \left(1 - \frac{T}{K}\right) - m_A T \frac{h_A}{T + h_A} - T \frac{1}{FRI} \frac{I(P,T)^\gamma}{h_I^\gamma + I(P,T)^\gamma} \quad (2)$$

with the fire intensity  $I(P,T)$  (-) defined as:

$$I(P,T) = C(T) \cdot SMI(P), \quad (3)$$

landscape continuity  $C(T)$  (-) as:

$$C(T) = \frac{h_C^\beta}{h_C^\beta + T^\beta} \quad (4)$$

and the soil moisture index  $SMI(P)$  (-) as:

$$SMI(P) = \frac{h_{SMI}^\alpha}{h_{SMI}^\alpha + P^\alpha} \quad (5)$$

For an explanation of the parameters, see Table 1.

## 2.2. Parameterization

We fitted the model on tree-cover data for tropical and subtropical South America (13°N–35°S; Fig. 1). We used the data of Hirota et al. (2011). These are average Climate Research Unit (CRU) precipitation data (the average of 1961–2002) at 0.5° resolution



(Mitchell and Jones, 2005) and MODIS Vegetation Continuous Field 3 tree-cover data (31 October 2000 to 9 December 2001) at  $0.01^\circ$  resolution (Hansen et al., 2003). However, we excluded human-used areas and water bodies from the data, as identified in the Global Land Cover 2000 (GLC2000) dataset (classes 16–18 and 20–23; Scheffer et al., 2012), using the R package ‘raster’. The probability distributions of tree cover in natural landscapes can be thought of as displaying the interplay between stable attractors and stochasticity in the system (Van Nes et al., 2012). Hence, we assume that fitting the model on the tree-cover modes captures the stable states of the system. To quantify the deviations to these stable states we calculated the adjusted  $R^2_{model}$  of the model. Comparing that to the adjusted  $R^2_{trimodal}$  of the three means of the modes gives an estimate of how well the model fits the trimodal tree-cover distribution (more details can be found in Appendix A).

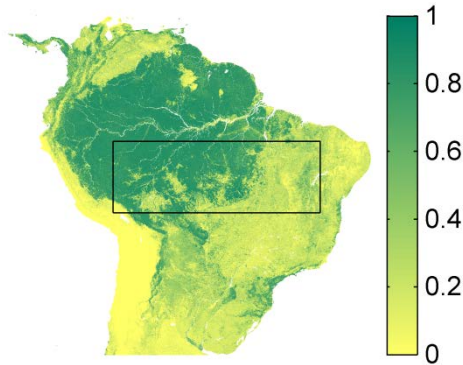


Figure 1: Tree cover (as a fraction) in tropical and subtropical South America. The total area shown was used for parameterizing the model ( $13^\circ\text{N}$ – $35^\circ\text{S}$ , but excluding human-used areas); the study area ( $5^\circ$ – $15^\circ\text{S}$ ,  $71^\circ$ – $42^\circ\text{W}$ ) is delineated. The data are at  $0.01^\circ$  resolution.

The parameterization of the model (Table 1) was done as follows. The logistic growth function from Van Nes et al. (2014) was kept intact, except for an adjustment of  $h_P$  to better match the tree-cover data at low precipitation values. No adjustments were made to the Allee-effect term, because we only fitted on the forest and savanna tree-cover values. In the fire

term, the half saturation for the soil moisture function  $h_{SMI}$  was based on Hirota et al. (2010).  $h_C$  is interpreted as the unstable threshold in tree cover between savanna and forest and should therefore approximately correspond to the least common tree-cover value between these modes in the South American tree-cover frequency distribution (0.56; Fig. A1). The fire return interval  $FRI$  was fine-tuned within a realistic range (3–10 years; Ratter, 1992). The remaining parameters, which are half saturation for fire intensity  $h_I$  and the exponents  $\alpha$ ,  $\beta$  and  $\gamma$  were fine-tuned without a predetermined range. This was done such that the model had a forest-savanna bistability range of approximately 1000–2500 mm yr<sup>-1</sup> (Fig. 2).

Table 1: The model's parameters and their values.

Parameter	Description	Value	Unit	Source
$\alpha$	Power in soil moisture index function	4	None	Fine-tuning
$\beta$	Power in continuity function	6	None	Fine-tuning
$\gamma$	Power in fire-induced mortality term	6	None	Fine-tuning
$FRI$	Fire return interval	7	yr	(Ratter, 1992)
$h_A$	Half saturation of Allee effect	0.10	Fractional tree cover	(Van Nes et al., 2014)
$h_C$	Half saturation of grass (non-forest) cover continuity	0.57	Fractional tree cover	This research
$h_I$	Half saturation of the fire-induced mortality term	0.15	None	Fine-tuning
$h_P$	Half saturation of growth term	80	mm yr <sup>-1</sup>	Fine-tuning
$h_{SMI}$	Half saturation of the soil	1800	mm yr <sup>-1</sup>	(Hirota et al.,

moisture index			2010)	
K	Maximum tree cover	0.90	Fractional tree cover	(Van Nes et al., 2014)
$m_A$	Mortality due to Allee effect	0.15	$\text{yr}^{-1}$	(Van Nes et al., 2014)
$r_m$	Maximum tree-cover growth rate	0.30	$\text{yr}^{-1}$	(Van Nes et al., 2014)

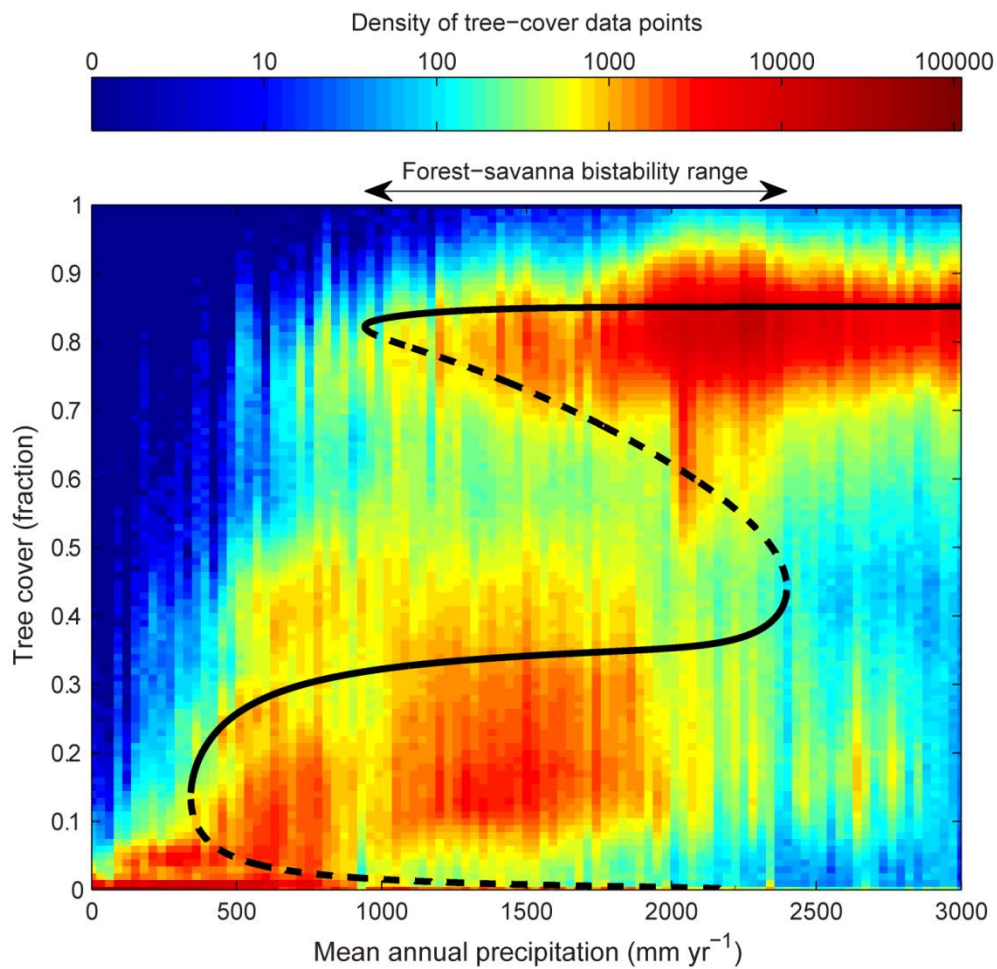


Figure 2: Equilibria of the model. The stable (solid lines) and unstable (dashed lines) equilibria of the model are shown with the background showing the frequency of tree-cover values from tropical and sub-tropical South America. The data at  $0.01^\circ$  resolution (Hirota et al., 2011) are displayed on a  $101 \times 101$  lattice. Only tree-cover values at locations with MAP

up to 3000 mm yr<sup>-1</sup> are shown (n = 8723784). Note the logarithmic scale along which the distribution of the data are presented.

### 2.3. Application

The study area to which the model was applied spans 15°–5°S latitude and 71°–42°W longitude (the delineated area in Fig. 1). It mostly covers Brazil, but it also includes the Bolivian part of the Amazon basin and a small part of Peru. This region was chosen to include the forest-savanna boundary in the south-eastern Amazon basin (Hirota et al., 2010) and thereby part of the arc of deforestation, where historical deforestation has been high (Coe et al., 2013). Continued deforestation can be expected for the near future, despite recent and projected increases in protected forest area (Malhi et al., 2008). The region also marks a transition from a dry to a humid tropical climate; an east-west precipitation gradient exists from roughly 800 mm yr<sup>-1</sup> to 2400 mm yr<sup>-1</sup> (Fig. A5). Most forest trees belong to evergreen species with limited resistance to fire (Hirota et al., 2010).

Because past disturbances have been severe in this region, regional tree cover may be out of equilibrium. As we were interested in how far from equilibrium and how close to a regime shift tree cover in the study area is, we did not exclude human-used areas here. With the unfiltered data we calculated the adjusted  $R^2$  of the model to compare it with that of the near-continental parameterization dataset. We then analyzed the occurrences of regime shifts from forest to savanna due to climate change and deforestation on a grid of cells representing the study area. This grid had the resolution of the precipitation data (0.5°). We considered spatial interactions (e.g. dispersion of trees) irrelevant on this scale. We resampled the tree-cover data from 0.01° to 0.5° resolution using the ArcGIS ‘majority’ resampling method. This method of resampling encompasses assigning the value to the output cell that is most abundant in the input cells. We assumed that the 2500 input cells per output cell are sufficient

to distinguish between the savanna, forest and treeless states. The choice for ‘majority’ prevents a bias towards average, unrealistic tree-cover values. For reasons of convenience, the resampled tree cover is called ‘observed’ in this paper. We ran the model with those observed values as initial conditions and imposed climate change and deforestation on the cells that have an observed tree cover of at least 0.60 and also stabilized at the forest state in the model.

Gradual climate change was simulated by decreasing MAP with steps of 0.01 times the measured value for each cell. At each step, observed tree cover was set as initial condition. Subsequently, tree cover of forest cells was reduced with steps of 0.01 (up to 0.30) times the observed cover to check when a shift to savanna took place resulting from deforestation. This simulation continued up to a precipitation reduction of 40%, which can be considered as an extreme scenario. The interaction effects of deforestation and drought on the occurrences of regime shifts were quantified as relative increases in the number of cells that shifted to the savanna state. A relative increase was calculated by dividing the total amount of shifted cells at a certain combination of deforestation and precipitation reduction by the amount of cells that had also shifted under either of the two perturbations. All simulations were performed using the GRIND for MATLAB (R2012b) software. Differential equations were solved with the Dormand Prince 4.5 solver (ode45) and all runs consisted of 1000 time steps.

### 3. Results

The parameterization resulted in a model with three stable tree-cover states: forest ( $T \approx 0.85$ ), savanna ( $0.20 \leq T \leq 0.40$ ) and a treeless state ( $T = 0$ ). Depending on mean annual precipitation, tree cover could be in either of one, two or three possible stable equilibria. Fire intensity starts decreasing sharply after  $T \approx 0.40$ , causing bistability of forest and savanna for a large precipitation range, from 950 to 2400 mm yr<sup>-1</sup>. This range is visually in agreement with the continental parameterization data (Fig. 2). The multi-modality in the data was not

determined by multi-modality in environmental variables (Appendix A). The precipitation range with bistability is wider than in the model of Van Nes et al. (2014) (1100–1600 mm yr<sup>-1</sup>). This difference results partly from the different parameterizations and partly from the different implementation of the fire-induced tree-cover mortality in the model of this paper (see Appendix D for a more elaborate comparison). The adjusted  $R^2_{trimodal}$  of the three means of the regimes was 0.96 and the model's adjusted  $R^2_{model}$  was 0.90 (Table S1). In the study area, the  $R^2_{model}$  was 0.81 (Table S3).

Resampling of the data in the study area did hardly affect the distributions of forest and savanna and the modes in the frequency distribution of tree cover (Fig. A3 and A4; Staver et al., 2011a). When the model was subsequently ran with those resampled data as initial conditions the equilibrium distributions of forest and savanna were consistent with the observations (Fig. 3). By performing model runs after initializing the grid at various tree-cover values ( $T = 0.85$  for forest, 0.30 for savanna and 0.01 for treeless), the geographical range of bistability and tristability could be determined (Fig. A6). In 4% of the cells forest was the only stable state. These cells were located in the state of Amazonas (in the block 5–6.5°S and 71–65.5°W), at the border of the states of Amazonas, Pará and Mato Grosso (7–8°S and 58.5–57.5°W) and in Peru near the Bolivian border (11–14°S and 71–69°W). In the remaining cells savanna was stable. Also, tree cover remained at the forest state in 94% of the cells, implying bistability of forest and savanna in 90% of the cells. This area extends as east as Piauí (approximately 44°W longitude). Tree cover decreased to a treeless state ( $T < 0.001$ ) in 13% of the cells. Thus, in 7% the cells tree cover stabilized at another state in all three runs.

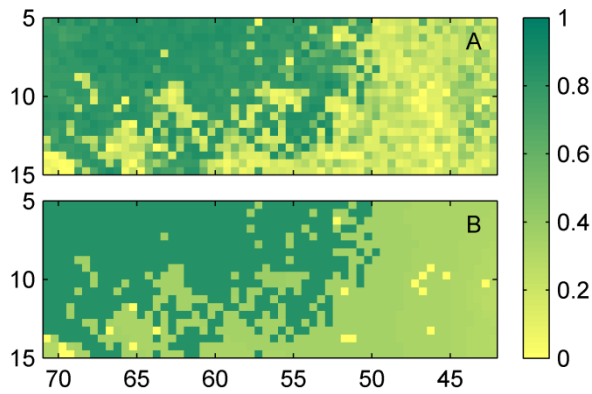


Figure 3: Tree cover in the study area at 0.5° resolution. A) Observed tree cover; and B) tree cover after stabilization in the model with the observed tree cover as initial conditions.

Reducing MAP in the cells with observed forest resulted in critical transitions to savanna (Fig. 4). At the most extreme scenario considered (40% reduction in MAP), 19% of the forested cells had shifted to savanna. A similar amount of cells (22%) had shifted in the absence of climate change at a deforestation of 20% tree cover per cell (Fig. 4). More than half of the forest (281 cells, being 51%) disappeared when 30% of the observed tree cover was subtracted from each cell. In combination, drought and deforestation tipped forested cells to the savanna state at lower levels of these perturbations than by themselves. Furthermore, more cells underwent a regime shift in the simulated ranges of the perturbations (Fig. 4). This interactive effect was most pronounced when precipitation reduction was between 20–40% and deforestation between 10–20%, when, on average, five times as many cells shifted than at the respective precipitation reduction and deforestation separately (Fig. A7). The largest interaction effect was found at a reduced MAP of 32% and deforestation of 14% at each cell, when 6.6 times as many shifts were observed.

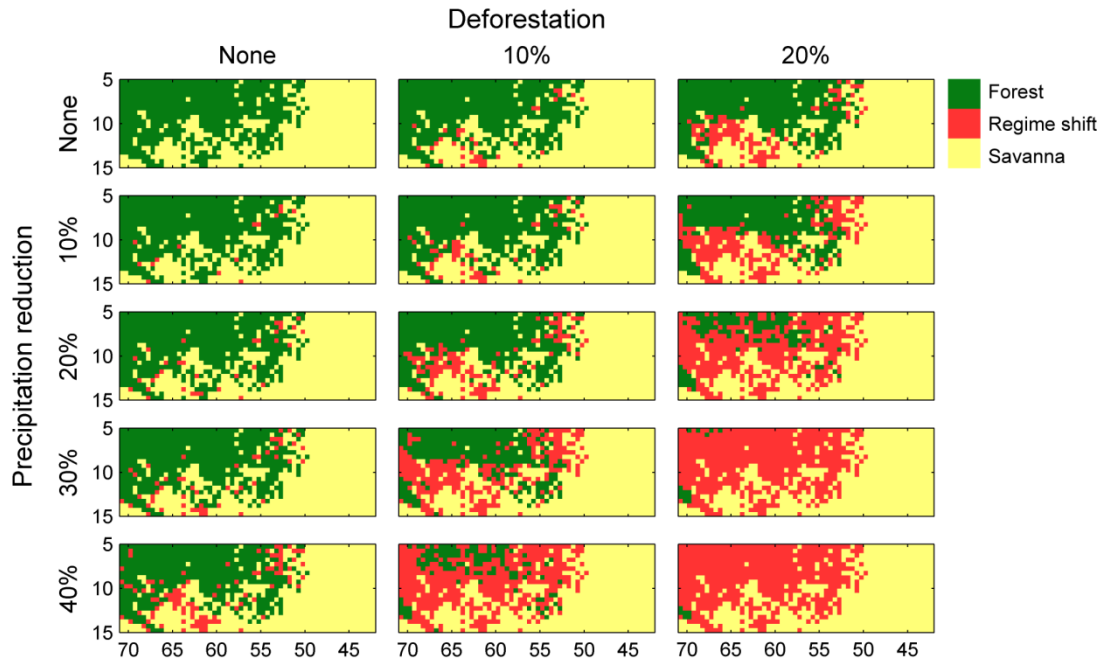


Figure 4: Regime shifts from forest to savanna at different levels of precipitation reduction and deforestation. The rows represent situations without precipitation reduction and with 10%, 20%, 30% and 40% reduction of current mean annual precipitation. The columns represent situations without deforestation and with removal of 10% and 20% of the observed tree cover. Green cells indicate locations where forest is predicted under the given conditions (MODIS tree cover without human-used areas excluded). Red cells indicate a predicted regime shift to a savanna ecosystem and light-yellow cells are already in a savanna (or treeless) regime.

#### 4. Discussion

We presented a simple model that has three alternative tree-cover states and was fitted on tree-cover data from tropical and sub-tropical South America. Due to a simple tree cover-fire feedback depending on climate the model has bistability of forest and savanna over a large range of mean annual precipitation (950–2400 mm yr<sup>-1</sup>). Our analysis using tree-cover and precipitation data from the south-eastern Amazon rainforest suggests a strong synergy



between drought and deforestation on the occurrence of regime shifts in this area. Drought, simulated as a reduction in mean annual precipitation (MAP), decreased the resilience of the forest state, thereby increasing the chance that a perturbation such as deforestation causes a shift to a savanna regime. Similarly, a perturbed forest was more likely to undergo a regime shift as a result of drought. Deforestation and drought interacted strongly because both increased fire intensity. How this interaction caused regime shifts is illustrated in Fig. 5, where a hypothesized combination of deforestation and drought pushes the system to the savanna basin of attraction. Separately, neither of the two would cause such a shift, due to the shape of the unstable equilibrium line. The synergy was strongest around 30–35% precipitation reduction and 15% deforestation, where the interaction effect accounted for over 80% of the regime shifts. This suggests that plausible levels of either deforestation or precipitation reduction could strongly increase the sensitivity of the south-eastern Amazon rainforest to the other if an unstable threshold is approached (Van Nes and Scheffer, 2003). However, most forest cells may undergo a shift due to deforestation even in the absence of a change in MAP, because they were bi- or tristable. On the other hand, in many cells a critical transition due to precipitation reduction occurred only in combination with deforestation, despite the finding that the forest may already be out of equilibrium.

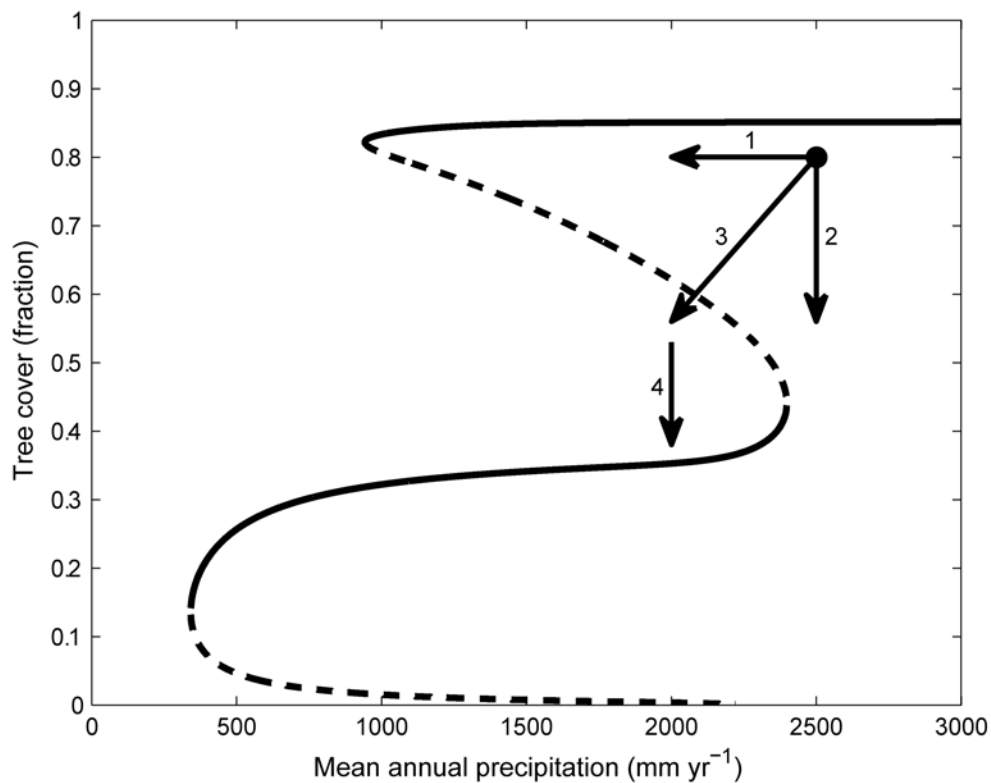


Figure 5: How the interaction between precipitation reduction and deforestation may cause a regime shift in the model. If in a forested area with  $T = 0.80$  at  $P = 2500 \text{ mm yr}^{-1}$  a decrease in precipitation of 20% takes place (1), no changes in the state of the system would be apparent, as the system is still in the basin of attraction of the forest state. However, savanna has become an alternate stable state, so a simultaneous deforestation of 30% (2) may push the system across the unstable equilibrium (3). The system then moves to the savanna state (4). Note that the position of a site relative to the unstable equilibrium line in the model determines at which combinations of precipitation reduction and deforestation the system undergoes regime shifts.

The modeled relationship between tree cover and fire intensity agrees with the empirical findings of Archibald et al. (2009) that fire becomes rare when tree cover exceeds 0.40. Thus, this feedback mechanism could plausibly cause the apparent forest-savanna bistability as

observed by Hirota et al. (2011) and Staver et al. (2011b). We were able to reproduce the statistical patterns of tree cover in South America, although we ignored factors such as the different response of savanna- and forest-tree species to fire. Nevertheless, this difference in response to fire is known to be an important factor in savanna dynamics (Hoffmann et al., 2012). Forest trees have much higher mortality rates in response to fire than savanna trees, but also have a competitive advantage over savanna trees under shaded conditions (Hoffmann et al., 2012). These differences between the functional types have been included in a simple model by Staver and Levin (2012). The same principle can be included in our model by adding a tree-cover equation for each of the two functional types. Such an addition could help incorporating tree-cover hysteresis in Dynamic Global Vegetation Models (DGVMs) that differentiate between these functional types. Often, such DGVMs insufficiently account for the tree cover-fire feedback (Baudena et al., 2014). One difficulty in parameterizing for various functional types in our type of model lies, however, in the fact that the tree-cover data aggregate all tree species. Essentially, only the percentage of area covered by woody species (tree cover) and the area covered by herbaceous species ( $1 - \text{tree cover}$ ) can be obtained. This is a limitation that causes a need for studies that relate tree-cover data to other biologically relevant variables. Recently, Yin et al. (2014) showed for West-Africa that the tree-cover bimodality coincides with aboveground biomass bimodality and inferred vegetation structure from these results. The low tree-cover mode had low biomass and consisted of savanna species (vertical structure) as well as of forest species (horizontal structure). The high tree-cover mode only consisted of forest species, but could have either high or low biomass (Yin et al., 2014).

We checked whether the bimodality in the tree-cover distribution could be explained by bimodality in annual temperature or precipitation, but this was not the case. Staver et al. (2011b) found, however, that at very strong rainfall seasonality forests are rarely found. This

is relevant, as an increase in dry-season length is expected for the south-eastern Amazon that may have profound effects on the forest (Fu et al., 2013). However, because savannas can be found in the tropics regardless of dry-season length (Staver et al., 2011b), weak seasonality would not prevent the regime shifts that our model predicts. Nevertheless, the inclusion of seasonality, as well as inter-annual precipitation variability (Holmgren et al., 2013), may be an interesting option for future explorations of the model.

Some possible biases in the data deserve mentioning. Firstly, a bias in the tree-cover data may lie in the algorithms used to generate the MODIS data. As Hanan et al. (2014) show, uniformly distributed tree cover may be reflected in an increased frequency of tree cover in the savanna range. We did not correct for this, and apart from excluding human-used areas used the same dataset as Hirota et al. (2011). Secondly, the hysteresis inferred by Staver et al. (2011b) and this study may be overestimated, as the large hysteresis suggested by the data may also be a manifestation of a range of smaller hysteresis loops resulting from heterogeneity in the landscape (e.g. regarding the soil; Van Nes et al., 2014). On the other hand, we did not consider any feedbacks in the climate, which may increase the bistability range. Although the exact relation between deforestation and precipitation is complex (Lawrence and Vandecar, 2015), we can expect that the regional positive forest-precipitation feedback in the Amazon (Oyama and Nobre, 2003; Zemp et al., 2014) would contribute to a deforestation-triggered transition to savanna. Because of such cross-scale interactions, linking feedbacks across scales would increase our understanding of the resilience of the system at landscape scale (Rietkerk et al., 2011).

In our model, the unstable threshold between the basins of attraction of forest and savanna that we attribute to fire is climate-dependent: at higher levels of MAP the resilience of the forest biome increases due to decreased fire intensity. Thus we provide regarding South America a more refined value for this threshold than Hirota et al. (2011), who suggested a

climate-insensitive unstable equilibrium at 60% tree cover. A climate-dependent unstable equilibrium accounts for interaction effects between precipitation reduction and deforestation on regime shifts. Hence, future modeling studies seeking a simple way to include the effects of possible local alternative stable states in Amazonian tree cover could benefit from the approach described here and in Van Nes et al. (2014). On a more applied level, our model predicts that deforestation in the south-eastern Amazon rainforest will result in regime shifts to savanna. Furthermore, degradation of the forest may cause it to become very vulnerable to anthropogenic climate change. Therefore, we endorse the need for policies that counteract deforestation in order to preserve the Amazon rainforest in a world under climate change.

**Acknowledgements** AS is supported by a PhD scholarship “Complex dynamics in human-environment systems” from SENSE Research School and EHvN is supported by an ERC grant that was awarded to Marten Scheffer. AS is grateful to Rafael Bernardi for his help on processing GLC2000 data and to Sebastian Bathiany for the display of an inspiring acknowledgement.

## References

- Aragão, L.E.O.C., Malhi, Y., Roman-Cuesta, R.M., Saatchi, S., Anderson, L.O., Shimabukuro, Y.E., 2007. Spatial patterns and fire response of recent Amazonian droughts. *Geophysical Research Letters* 34, L07701.
- Archibald, S., Roy, D.P., van Wilgen, B.W., Scholes, R.J., 2009. What limits fire? An examination of drivers of burnt area in Southern Africa. *Global Change Biology* 15, 613-630.
- Baudena, M., D'Andrea, F., Provenza, A., 2010. An idealized model for tree–grass coexistence in savannas: the role of life stage structure and fire disturbances. *Journal of Ecology* 98, 74-80.
- Baudena, M., Dekker, S.C., van Bodegom, P.M., Cuesta, B., Higgings, S.I., Lehsten, V., Reick, C.H., Rietkerk, M., Scheiter, S., Yin, Z., Zavala, M.A., Brovkin, V., 2014. Forests, savannas and grasslands: bridging the knowledge gap between ecology and Dynamic Global Vegetation Models. *Biogeosciences Discussions* 11, 9471-9510.
- Bond, W.J., 2008. What limits trees in C4 grasslands and savannas? *Annual Review of Ecology, Evolution, and Systematics* 39, 641-659.
- Brando, P.M., Balch, J.K., Nepstad, D.C., Morton, D.C., Putz, F.E., Coe, M.T., Silvério, D., Macedo, M.N., Davidson, E.A., Nóbrega, C.C., Alencar, A., Soares-Filho, B.S., 2014. Abrupt increases in Amazonian tree mortality due to drought–fire interactions. *Proceedings of the National Academy of Sciences* 111, 6347-6352.
- Bucini, G., Hanan, N.P., 2007. A continental-scale analysis of tree cover in African savannas. *Global Ecology and Biogeography* 16, 593-605.

426 Cochrane, M.A., Alencar, A., Schulze, M.D., Souza Jr, C.M., Nepstad, D.C., Lefebvre, P.,  
 427 Davidson, E.A., 1999. Positive feedbacks in the fire dynamic of closed canopy tropical  
 428 forests. *Science* 284, 1832-1835.

429 Coe, M.T., Marthews, T.R., Costa, M.H., Galbraith, D.R., Greenglass, N.L., Imbuzeiro,  
 430 H.M.A., Levine, N.M., Malhi, Y., Moorcroft, P.R., Muza, M.N., Powell, T.L., Saleska, S.R.,  
 431 Solorzano, L.A., Wang, J., 2013. Deforestation and climate feedbacks threaten the ecological  
 432 integrity of south-southeastern Amazonia. *Philosophical Transactions of the Royal Society B:*  
 433 *Biological Sciences* 368, 20120155.

434 Cox, P.M., Betts, R.A., Jones, C.D., Spall, S.A., Totterdell, I.J., 2000. Acceleration of global  
 435 warming due to carbon-cycle feedbacks in a coupled climate model. *Nature* 408, 184-187.

436 Cumming, G.S., Southworth, J., Rondon, X.J., Marsik, M., 2012. Spatial complexity in  
 437 fragmenting Amazonian rainforests: Do feedbacks from edge effects push forests towards an  
 438 ecological threshold? *Ecological Complexity* 11, 67-74.

439 Davidson, E.A., De Araújo, A.C., Artaxo, P., Balch, J.K., Brown, I.F., C. Bustamante, M.M.,  
 440 Coe, M.T., Defries, R.S., Keller, M., Longo, M., Munger, J.W., Schroeder, W., Soares-Filho,  
 441 B.S., Souza Jr, C.M., Wofsy, S.C., 2012. The Amazon basin in transition. *Nature* 481, 321-  
 442 328.

443 Farr, T.G., Rosen, P.A., Caro, E., Crippen, R., Duren, R., Hensley, S., Kobrick, M., Paller,  
 444 M., Rodriguez, E., Roth, L., 2007. The shuttle radar topography mission. *Reviews of*  
 445 *Geophysics* 45, RG2004.

446 Fu, R., Yin, L., Li, W., Arias, P.A., Dickinson, R.E., Huang, L., Chakraborty, S., Fernandes,  
 447 K., Liebmann, B., Fisher, R., Myneni, R.B., 2013. Increased dry-season length over southern  
 448 Amazonia in recent decades and its implication for future climate projection. *Proceedings of*  
 449 *the National Academy of Sciences* 110, 18110-18115.

450 Gil-Romera, G., Lamb, H.F., Turton, D., Sevilla-Callejo, M., Umer, M., 2010. Long-term  
 451 resilience, bush encroachment patterns and local knowledge in a Northeast African savanna.  
 452 *Global environmental change* 20, 612-626.

453 Hanan, N.P., Tredennick, A.T., Prihodko, L., Bucini, G., Dohn, J., 2014. Analysis of stable  
 454 states in global savannas: is the CART pulling the horse? *Global Ecology and Biogeography*  
 455 23, 259-263.

456 Hansen, M., DeFries, R., Townshend, J., Carroll, M., Dimiceli, C., Sohlberg, R., 2003. Global  
 457 percent tree cover at a spatial resolution of 500 meters: First results of the MODIS vegetation  
 458 continuous fields algorithm. *Earth Interactions* 7, 1-15.

459 Hirota, M., Holmgren, M., Van Nes, E.H., Scheffer, M., 2011. Global resilience of tropical  
 460 forest and savanna to critical transitions. *Science* 334, 232-235.

461 Hirota, M., Nobre, C., Oyama, M.D., Bustamante, M.M.C., 2010. The climatic sensitivity of  
 462 the forest, savanna and forest-savanna transition in tropical South America. *New Phytologist*  
 463 187, 707-719.

464 Hoffmann, W.A., Geiger, E.L., Gotsch, S.G., Rossatto, D.R., Silva, L.C., Lau, O.L.,  
 465 Haridasan, M., Franco, A.C., 2012. Ecological thresholds at the savanna-forest boundary:



466 how plant traits, resources and fire govern the distribution of tropical biomes. *Ecology Letters*  
467 15, 759-768.

468 Holling, C.S., 1973. Resilience and stability of ecological systems. *Annual Review of*  
469 *Ecology and Systematics* 4, 1-23.

470 Holmgren, M., Hirota, M., Van Nes, E.H., Scheffer, M., 2013. Effects of interannual climate  
471 variability on tropical tree cover. *Nature Climate Change* 3, 755-758.

472 Holmgren, M., Scheffer, M., Huston, M.A., 1997. The interplay of facilitation and  
473 competition in plant communities. *Ecology* 78, 1966-1975.

474 Lawrence, D., Vandecar, K., 2015. Effects of tropical deforestation on climate and  
475 agriculture. *Nature Climate Change* 5, 27-36.

476 Lenton, T.M., Held, H., Kriegler, E., Hall, J.W., Lucht, W., Rahmstorf, S., Schellnhuber, H.J.,  
477 2008. Tipping elements in the Earth's climate system. *Proceedings of the National Academy*  
478 *of Sciences* 105, 1786-1793.

479 Malhi, Y., Aragão, L.E.O.C., Galbraith, D., Huntingford, C., Fisher, R., Zelazowski, P., Sitch,  
480 S., McSweeney, C., Meir, P., 2009. Exploring the likelihood and mechanism of a climate-  
481 change-induced dieback of the Amazon rainforest. *Proceedings of the National Academy of*  
482 *Sciences* 106, 20610-20615.

483 Malhi, Y., Roberts, J.T., Betts, R.A., Killeen, T.J., Li, W., Nobre, C.A., 2008. Climate  
484 change, deforestation, and the fate of the Amazon. *Science* 319, 169-172.

485 Mitchell, T.D., Jones, P.D., 2005. An improved method of constructing a database of monthly  
 486 climate observations and associated high-resolution grids. *International Journal of*  
 487 *Climatology* 25, 693-712.

488 Moreira, A.G., 2000. Effects of fire protection on savanna structure in central Brazil. *Journal*  
 489 *of Biogeography* 27, 1021-1029.

490 Murphy, B.P., Bowman, D.M.J.S., 2012. What controls the distribution of tropical forest and  
 491 savanna? *Ecology Letters* 15, 748-758.

492 Nepstad, D.C., Stickler, C.M., Soares-Filho, B., Merry, F., 2008. Interactions among Amazon  
 493 land use, forests and climate: Prospects for a near-term forest tipping point. *Philosophical*  
 494 *Transactions of the Royal Society B: Biological Sciences* 363, 1737-1746.

495 Nobre, C.A., Borma, L.D.S., 2009. 'Tipping points' for the Amazon forest. *Current Opinion in*  
 496 *Environmental Sustainability* 1, 28-36.

497 Oyama, M.D., Nobre, C.A., 2003. A new climate-vegetation equilibrium state for tropical  
 498 South America. *Geophysical Research Letters* 30, 2199.

499 Pueyo, S., de Alencastro Graça, P.M.L., Barbosa, R.I., Cots, R., Cardona, E., Fearnside, P.M.,  
 500 2010. Testing for criticality in ecosystem dynamics: The case of Amazonian rainforest and  
 501 savanna fire. *Ecology Letters* 13, 793-802.

502 Ratter, J.A., 1992. Transitions between cerrado and forest vegetation in Brazil, in: Furley,  
 503 P.A., Proctor, A., Ratter, J.A. (Eds.), *Nature and dynamics of forest-savanna boundaries*.  
 504 Chapman and Hall, London, pp. 417-429.

505 Reyer, C.P.O., Brouwers, N., Rammig, A., Brook, B.W., Epila, J., Grant, R.F., Holmgren, M.,  
 506 Langerwisch, F., Leuzinger, S., Lucht, W., Medlyn, B., Pfeifer, M., Steinkamp, J.,  
 507 Vanderwel, M.C., Verbeeck, H., Vilella, D.M., 2015. Forest resilience and tipping points at  
 508 different spatio-temporal scales: approaches and challenges. *Journal of Ecology* 103, 5-15.

509 Rietkerk, M., Brovkin, V., van Bodegom, P.M., Claussen, M., Dekker, S.C., Dijkstra, H.A.,  
 510 Goryachkin, S.V., Kabat, P., van Nes, E.H., Neutel, A.M., Nicholson, S.E., Nobre, C.,  
 511 Petoukhov, V., Provenzale, A., Scheffer, M., Seneviratne, S.I., 2011. Local ecosystem  
 512 feedbacks and critical transitions in the climate. *Ecological Complexity* 8, 223-228.

513 Sankaran, M., Hanan, N.P., Scholes, R.J., Ratnam, J., Augustine, D.J., Cade, B.S., Gignoux,  
 514 J., Higgins, S.I., Le Roux, X., Ludwig, F., Ardo, J., Banyikwa, F., Bronn, A., Bucini, G.,  
 515 Caylor, K.K., Coughenour, M.B., Diouf, A., Ekaya, W., Feral, C.J., February, E.C., Frost,  
 516 P.G.H., Hiernaux, P., Hrabar, H., Metzger, K.L., Prins, H.H.T., Ringrose, S., Sea, W., Tews,  
 517 J., Worden, J., Zambatis, N., 2005. Determinants of woody cover in African savannas. *Nature*  
 518 438, 846-849.

519 Scheffer, M., 2009. *Critical Transitions in Nature and Society*. Princeton University Press,  
 520 Princeton.

521 Scheffer, M., Bascompte, J., Brock, W.A., Brovkin, V., Carpenter, S.R., Dakos, V., Held, H.,  
 522 Van Nes, E.H., Rietkerk, M., Sugihara, G., 2009. Early-warning signals for critical  
 523 transitions. *Nature* 461, 53-59.

524 Scheffer, M., Carpenter, S.R., 2003. Catastrophic regime shifts in ecosystems: Linking theory  
 525 to observation. *Trends in Ecology and Evolution* 18, 648-656.

526 Scheffer, M., Hirota, M., Holmgren, M., Van Nes, E.H., Chapin Iii, F.S., 2012. Thresholds for  
 527 boreal biome transitions. *Proceedings of the National Academy of Sciences* 109, 21384-  
 528 21389.

529 Staver, A.C., Archibald, S., Levin, S., 2011a. Tree cover in sub-Saharan Africa: rainfall and  
 530 fire constrain forest and savanna as alternative stable states. *Ecology* 92, 1063-1072.

531 Staver, A.C., Archibald, S., Levin, S.A., 2011b. The global extent and determinants of  
 532 savanna and forest as alternative biome states. *Science* 334, 230-232.

533 Staver, A.C., Levin, S.A., 2012. Integrating theoretical climate and fire effects on savanna and  
 534 forest systems. *The American Naturalist* 180, 211-224.

535 Sternberg, L.S.L., 2001. Savanna-forest hysteresis in the tropics. *Global Ecology and*  
 536 *Biogeography* 10, 369-378.

537 Uhl, C., Kauffman, J.B., 1990. Deforestation, fire susceptibility, and potential tree responses  
 538 to fire in the eastern Amazon. *Ecology* 71, 437-449.

539 Van Nes, E.H., Hirota, M., Holmgren, M., Scheffer, M., 2014. Tipping points in tropical tree  
 540 cover: linking theory to data. *Global Change Biology* 20, 1016-1021.

541 Van Nes, E.H., Holmgren, M., Hirota, M., Scheffer, M., 2012. Response to comment on  
 542 "Global resilience of tropical forest and savanna to critical transitions". *Science* 336, 541-d.

543 Van Nes, E.H., Scheffer, M., 2003. Alternative attractors may boost uncertainty and  
 544 sensitivity in ecological models. *Ecological Modelling* 159, 117-124.

545 Yin, Z., Dekker, S., van den Hurk, B., Dijkstra, H., 2014. Bimodality of woody cover and  
546 biomass across the precipitation gradient in West Africa. *Earth System Dynamics* 5, 257-270.

547 Zemp, D.C., Schleussner, C.F., Barbosa, H.M.J., van der Ent, R.J., Donges, J.F., Heinke, J.,  
548 Sampaio, G., Rammig, A., 2014. On the importance of cascading moisture recycling in South  
549 America. *Atmospheric Chemistry and Physics* 14, 13337-13359.

550

## Appendix A. Trimodal tree cover and the model's goodness-of-fit

The frequency distribution of tree cover in tropical and subtropical South America (13°N–35°S; excluding human-used areas) is trimodal (Fig. A1).

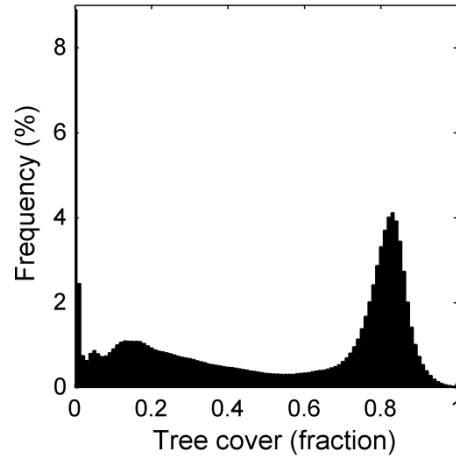


Fig. A1: The frequency distribution of the tree-cover data used for parameterizing the model (n = 9293107).

Fig. A2 shows that the trimodality in tree cover does not result from multimodality in mean annual precipitation (MAP) and mean annual temperature. Data points were divided into treeless, savanna and forest based on the minima of the frequency distribution of tree cover. These were 0.04 and 0.56 (Fig. A1), so the three groups (or regimes) were determined as  $0 \leq T \leq 0.04$  (treeless),  $0.05 \leq T \leq 0.56$  (savanna) and  $0.57 \leq T \leq 1$  (forest). The mean annual temperature for each  $0.5^\circ$  cell in the study area was determined by averaging monthly Climate Research Unit data from 1960–2000 (Mitchell and Jones, 2005). The cells were reshaped to  $0.01^\circ$  in MATLAB R2012b.

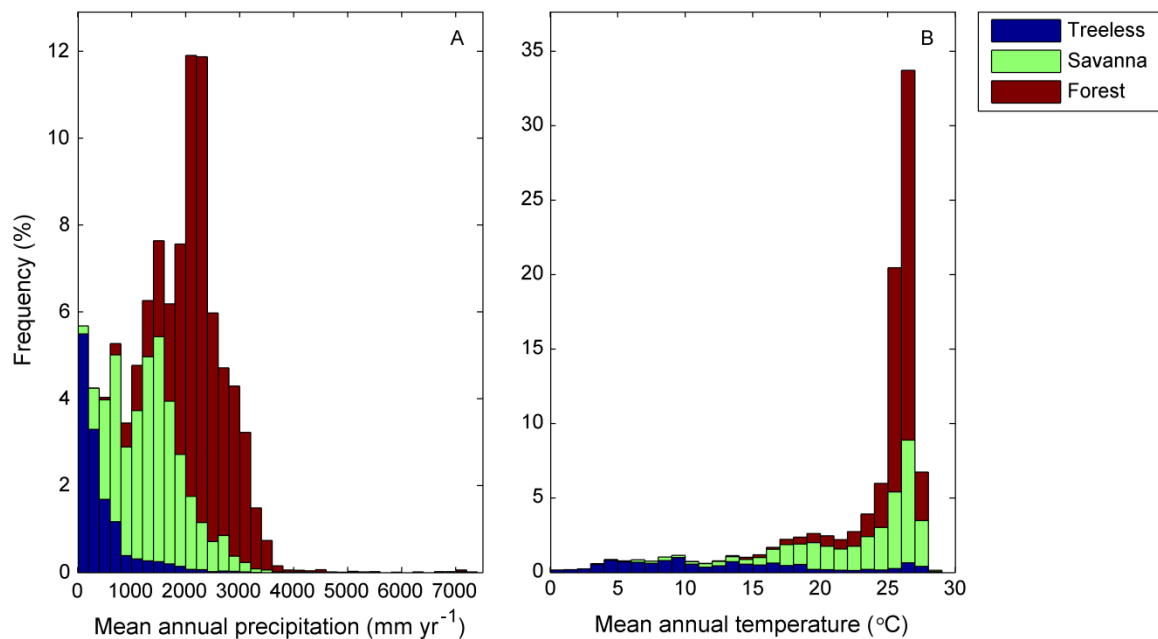


Fig. A2: Histograms of mean annual precipitation (A) and mean annual temperature (B) in tropical and subtropical South America with the distribution of treeless, savanna and forest regimes indicated.

We ran the model for five samples of 1000 data points until equilibrium. We then determined the deviations of the initial values (MODIS observations) to the stable outcomes of the run. We computed for each sample the adjusted  $R^2$ , whereby we adjusted for the seven fitted parameters in the model ( $\alpha$ ,  $\beta$ ,  $\gamma$ ,  $FRI$ ,  $h_C$ ,  $h_I$  and  $h_P$ ). However, to estimate the goodness-of-fit to a trimodal tree-cover distribution we wanted to compare the adjusted  $R^2_{model}$  to that of an ‘optimal model’ with three possible predictions. Therefore, we also calculated the  $R^2_{trimodal}$  of the means of the three regimes, again where  $0 \leq T \leq 0.04$  was treeless,  $0.05 \leq T \leq 0.56$  savanna and  $0.57 \leq T \leq 1$  was considered forest. We adjusted  $R^2_{trimodal}$  for the three means. The average  $R^2_{trimodal}$  of the samples ( $R^2 = 0.96$ ) was higher than the average  $R^2_{model}$  ( $R^2 = 0.90$ ) (Table A1).

Table A1: The adjusted  $R^2_{trimodal}$  of the means of the three modes to sampled data points (five independent sample of 1000) and the adjusted  $R^2_{model}$  of the model to those data points. Values in boldface are averages.

Sample	Adj. $R^2_{trimodal}$	Adj. $R^2_{model}$
1	0.964	0.897
2	0.962	0.908
3	0.963	0.909
4	0.963	0.888
5	0.963	0.900
	<b>0.963</b>	<b>0.900</b>

## Appendix B. Data from the study area

The frequency distribution of the tree cover data (at  $0.01^\circ$  resolution; Hirota et al., 2011) in the study area has two clear modes for savanna ( $T = 0.17$ ) and forest ( $T = 0.83$ ) as well as a small one for treeless ( $T = 0$ ) (Fig. B1A). The minima between these modes are at  $T = 0.03$  and  $T = 0.64$ . Resampling hardly affects the positioning and shape of the modes (Staver et al., 2011a). After converting the cells from  $0.01^\circ$  to  $0.5^\circ$  in which each  $0.5^\circ$  cell was given the most frequently occurring value out of 2500 cells at  $0.01^\circ$ , modes were located at  $T = 0.17$  and  $T = 0.81$ ;  $T = 0$  is not present after resampling (Fig. B1B). Of the resampled cells, 1% (14 out of a total of 1160) was entirely treeless, 51% (587 in total) had tree cover up to 0.60 and 48% (559) were forested. Both before and after resampling, forest was found to exist mainly in areas with  $MAP > 1300 \text{ mm yr}^{-1}$ . Savanna is present up until about  $2300 \text{ mm yr}^{-1}$  (Fig. B2).

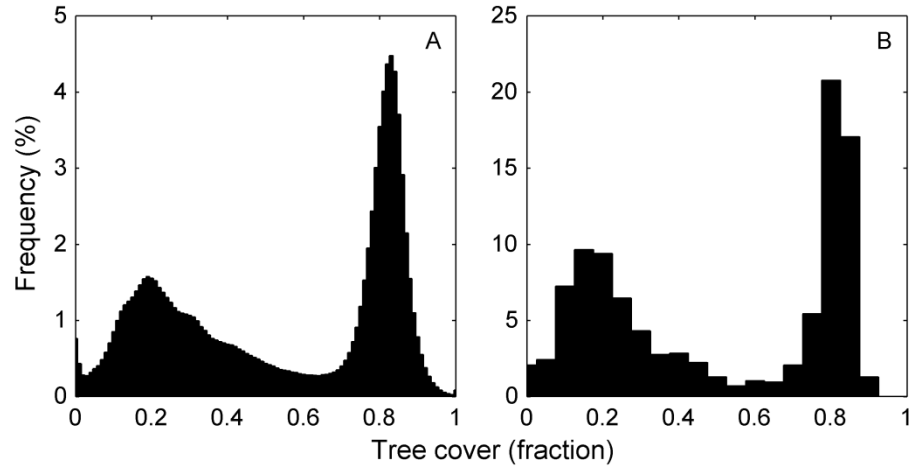


Fig. B1: Histograms of tree cover in the study area at (A)  $0.01^\circ$  resolution; and (B) after resampling to  $0.5^\circ$  resolution.

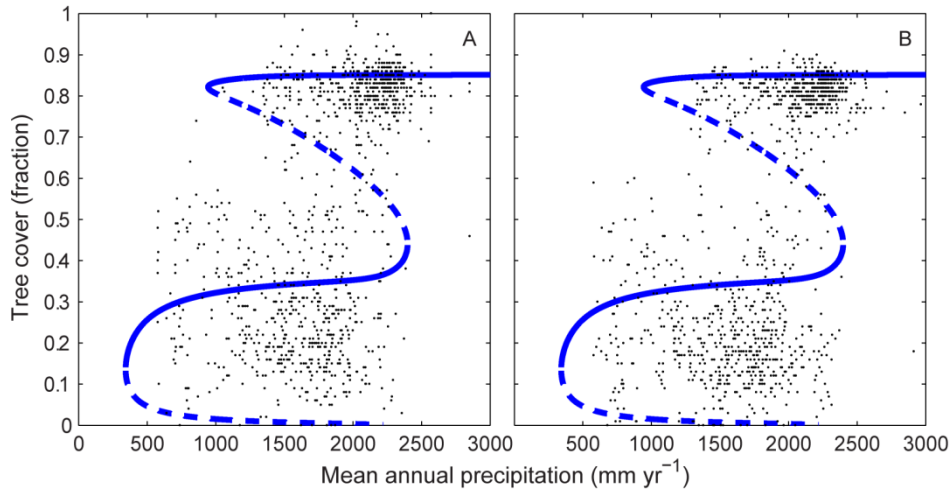


Fig. B2: Stable (solid lines) and unstable (dashed lines) equilibria with (A) a sample of 1152 data points at  $0.01^\circ$  resolution from the study area; and (B) with all 1152 resampled data points from the study area in the MAP range  $0\text{--}3000\text{ mm yr}^{-1}$ .

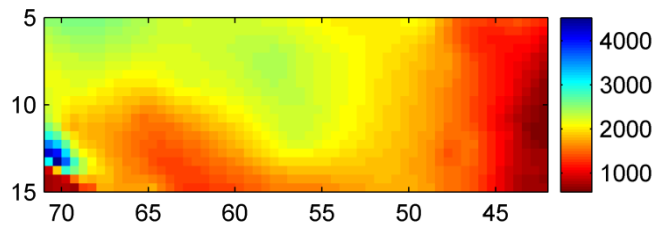


Fig. B3: Mean annual precipitation ( $\text{mm yr}^{-1}$ ) in the study area.

We checked how tree cover in the study area relates to environmental variables. Besides MAP (Fig. B3) and temperature, we considered landscape elevation. Elevation data taken from the NASA Shuttle Radar Topography Mission (Farr et al., 2007). These data are at 3 arcsecond resolution and were therefore averaged to  $0.01^\circ$  (i.e. 144 values were averaged to one). Any missing values in the original data were ignored. Regressions between these variables were performed in SPSS 21 with five independent samples of 1000 data points. MAP is strongly correlated to tree cover ( $R^2 = 0.31$ ). Elevation is moderately negatively correlated to tree



cover ( $R^2 = 0.09$ ) and mean annual temperature is weakly correlated to tree cover ( $R^2 = 0.03$ ) (Table B1).

Table B1: Pearson's  $R^2$  between elevation, mean annual temperature, mean annual precipitation and tree cover for the study area at  $0.01^\circ$  resolution. The results are of samples of 1000 out of 2872105 data points (681984 for correlations with elevation) and are highly significant ( $p \ll 0.01$ ). Values in boldface are averages.

	Temperature	Precipitation	Tree cover
Elevation	0.874	0.139	0.077
	0.878	0.125	0.088
	0.895	0.149	0.105
	0.857	0.142	0.076
	0.803	0.144	0.092
	<b>0.861</b>	<b>0.140</b>	<b>0.088</b>
Temperature		0.031	0.030
		0.038	0.027
		0.043	0.032
		0.028	0.033
		0.016	0.014
		<b>0.031</b>	<b>0.027</b>
Precipitation			0.350
			0.291
			0.292
			0.334
			0.274
			<b>0.308</b>

### Appendix C. Stability of tree cover in the study area

We also calculated the adjusted  $R^2_{model}$  in the study area (Table C1). The average of five samples is  $R^2 = 0.81$ , which is lower than in the parameterization dataset ( $R^2 = 0.90$ ).

Table C1: The adjusted  $R^2_{model}$  of the model to sampled data points (five independent sample of 1000) from the study area. The values in boldface is an average.

Sample	Adj. $R^2_{model}$
1	0.793
2	0.821
3	0.828
4	0.802
5	0.815
	<b>0.812</b>

Fig. C1 shows the distribution of the three ecosystem states in the study area after initializing the entire grid at: 1) forest ( $T = 0.85$ ); 2) savanna ( $T = 0.30$ ); and 3) treeless ( $T = 0.01$ ).

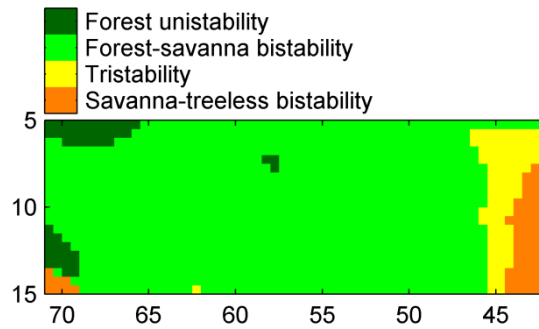


Fig. C1: Stable states after different tree cover initializations.

The interaction effect between deforestation and precipitation reduction was quantified as the relative increase in the number of regime shifts at a certain combination of the two compared to the number of shifts at deforestation and precipitation reduction separately. Fig. C2 visualizes how this interaction effect depends on the extent of precipitation reduction and deforestation for the 547 forest cells ( $0.5^\circ$  resolution) in the study area.

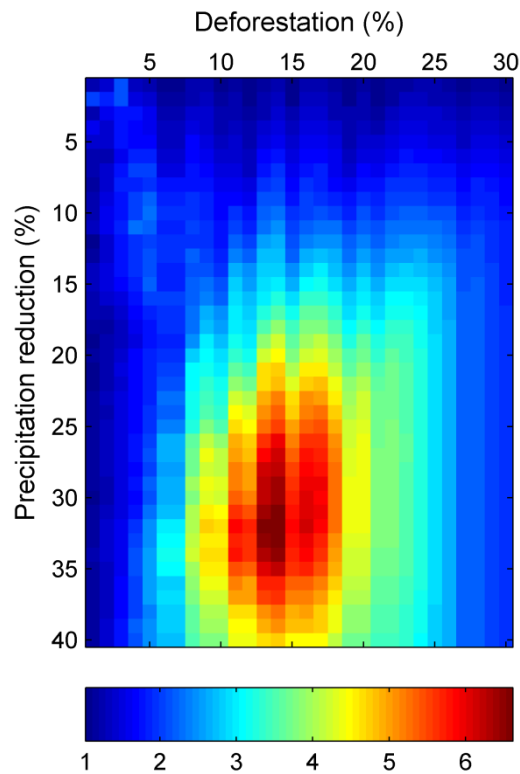


Fig. C2: The interaction effect between deforestation and precipitation reduction on the occurrence of regime shifts in the study area. The numbers indicate the relative increase in the number of regime shifts compared to the number of shifts at the respective deforestation and precipitation reduction separately.

#### Appendix D. Comparison with the Van Nes et al. (2014) model

Using the names and abbreviations of the parameters and variables from this paper, the Van Nes et al. (2014) model can be phrased as follows:

$$\frac{dT}{dt} = \frac{P}{h_P + P} r_m T \left(1 - \frac{T}{K}\right) - m_A T \frac{h_A}{T + h_A} - T \frac{1}{FRI} \frac{h_C^\beta}{h_C^\beta + T^\beta} \quad (D1)$$

and in its original form is parameterized as in Table D1.

Table D1: Parameterization of Van Nes et al. (2014). For comparison, the names, descriptions and units of this paper are retained.

Parameter	Description	Value	Unit
$\beta$	Power in continuity function	7	None
FRI	Fire return interval	1 / 0.11	yr
$h_A$	Half saturation of Allee effect	0.10	Fractional tree cover
$h_C$	Half saturation of grass (non-forest) cover continuity	0.64	Fractional tree cover
$h_P$	Half saturation of growth term	182.5	mm yr <sup>-1</sup>
K	Maximum tree cover	0.90	Fractional tree cover
$m_A$	Mortality due to Allee effect	0.15	yr <sup>-1</sup>
$r_m$	Maximum tree-cover growth rate	0.30	yr <sup>-1</sup>

The forest-savanna hysteresis of the Van Nes et al. (2014) model is 1100–1600 mm yr<sup>-1</sup>, smaller than of the paper presented in this paper (Fig. D1). When the Van Nes et al. (2014) model is parameterized as Table 1 (i.e. the fire-induced mortality only depends on  $T$ ) it has a bistability range of 350–1500 mm yr<sup>-1</sup> (with forest also stable between 250–350 mm yr<sup>-1</sup>). If this fire mortality term is multiplied by the soil moisture index, tree-cover mortality due to fire effectively equals annual fire intensity times tree cover. Performing this multiplication results in a bistability range of 350–850 mm yr<sup>-1</sup>. In the eventual model, tree cover is made resistant to low-intensity fires by incorporating a Hill function. Because this Hill function allows fire-induced tree-cover mortality to approach 1 (divided by  $FRI$ ) when intensity is considerably larger than half saturation  $h_I$ , higher mortality is possible than without this function. When the exponent  $\gamma$  is set to 1, tree cover increases with MAP without forest and savanna being alternative stable states. Bistability and hysteresis arise when  $\gamma$  exceeds approximately 1.34 (a fold bifurcation appears at 2040 mm yr<sup>-1</sup>). At higher  $\gamma$  hysteresis widens, with a forest-savanna bistability at 950–2400 mm yr<sup>-1</sup> at  $\gamma = 6$ .

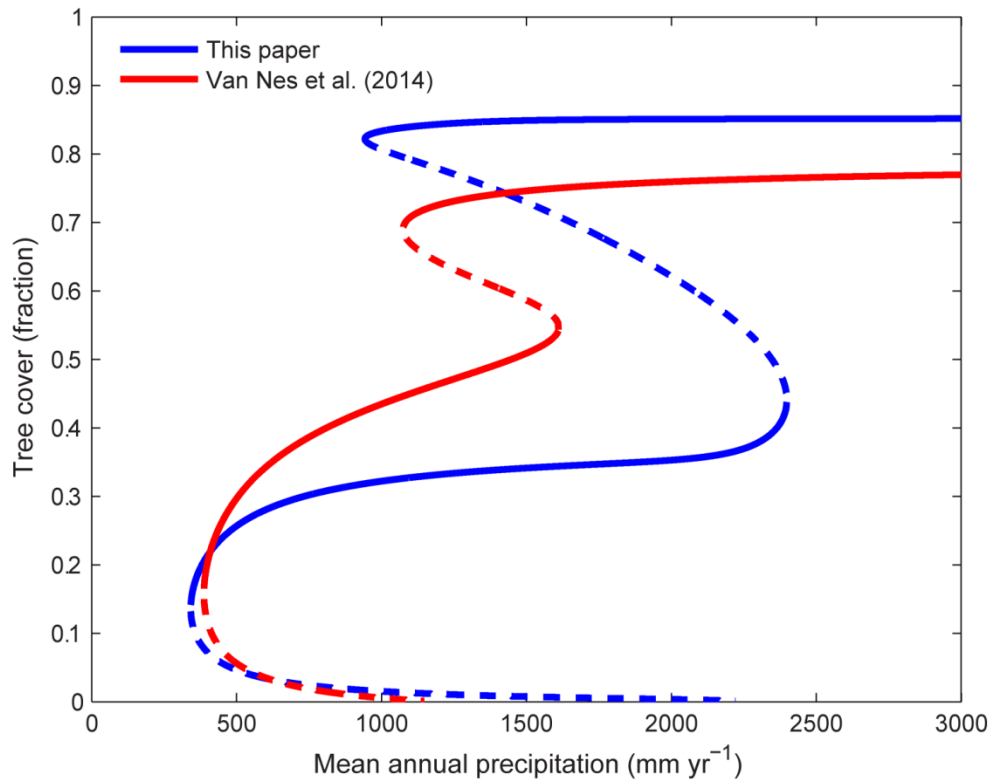


Fig. D1: The stable (solid lines) and unstable (dashed lines) tree-cover equilibria of the model presented in this paper and in Van Nes et al. (2014).

## Appendix E. Sensitivity analysis of the model

With a sensitivity analysis on the parameters it is observed how strongly the precipitation range at which both forest and savanna are stable is affected. Largest sensitivity was found on  $h_c$  and  $K$ , lowest on  $h_p$  (Table E1).

Table E1: Sensitivity analysis of the model, showing the ranges of mean annual precipitation at which forest and savanna are both stable (rounded at 50 mm yr<sup>-1</sup> and the treeless state not accounted for). At the default parameter settings the bistable range is 950–2400 mm yr<sup>-1</sup>.

Parameter	Value	-20%	-10%	+10%	+20%
$\alpha$	4	850-2550	900-2450	1000-2350	1050-2300
$\beta$	6	1550-2350	1350-2350	250-2400	150-2450
$\gamma$	6	1200-2350	1100-2350	800-2400	650-2450
FRI	7	1050-2550*	1000-2500	900-2300	850-2200
$h_A$	0.10	750-2350	850-2400	1050-2400	1100-2450
$h_c$	0.57	50-2150	100-2300	1700-2450	2050-2550
$h_I$	0.15	1350-2550	1200-2500	550-2300	300-2250
$h_{SMI}$	1800	800-1900	850-2150	1050-2650	1150-2850
$K$	0.90	2250-2550	1750-2500	100-2300	50-2150
$m_A$	0.15	700-2300	850-2350	1050-2400	1150-2450
$r_m$	0.30	1250-2600**	1100-2500	800-2300	600-2200

\* Savanna is only stable above 1500 mm yr<sup>-1</sup>. \*\* Savanna is only stable above 2400 mm yr<sup>-1</sup>.